Quantum Electronics **49** (7) 689–692 (2019)

TERAHERTZ RADIATION

https://doi.org/10.1070/QEL16892

Generation of THz radiation at a difference frequency in a HgCdTe-based laser

A.A. Dubinov, V.Ya. Aleshkin, S.V. Morozov

Abstract. **The results of a theoretical study of THz radiation generation at a difference frequency in a HgTe/HgCdTe quantum-well laser are presented. It is shown that in such a laser having a waveguide width of 100 μm, at the power 1 W of the near-IR radiation modes the radiation power at the difference frequency in the range 0.5–3.5 THz reaches 90 μW at room temperature.**

Keywords: *laser, THz frequency range, difference frequency.*

1. Introduction

The development of compact solid-state radiation sources operating in the THz frequency range (1–10 THz) is one of the most important goals of modern semiconductor physics. Such radiation sources are in demand for many applications, primarily for the spectroscopy of gases and solids, environmental monitoring and medicine [1–3]. In the long-wavelength part of the THz frequency range (1–5 THz), monopolar quantum cascade lasers based on GaAs and InP occupy the leading place among semiconductor lasers, but they operate only at cryogenic temperatures [4]. Thus, the problem of fabricating a compact THz radiation source operating at room temperature remains important.

Promising sources of THz radiation at room temperature can be based on intracavity nonlinear optical conversion (difference frequency generation) of radiation at two wavelengths of the near or middle IR range. Earlier, Aleshkin et al. [5] theoretically considered the possibility of generating a difference frequency due to the lattice nonlinearity of GaAs [6] in an interband two-frequency near-IR laser containing two different InGaAs/GaAs quantum wells in the active region. The main difficulty in obtaining efficient difference frequency generation is the need to satisfy the phase matching condition. For GaAs, it is well known [7, 8] that if the shortest wavelength in the near-IR range is smaller than a certain critical wavelength ($\lambda < \lambda_c$), then it is impossible to satisfy this condition for generating a difference frequency below 3 THz (where there the phonon absorption is small). The fact is that for $\lambda < \lambda_c$, due to the normal dispersion of the semiconductor refractive index, the phase velocity of the nonlinear polarisation wave is lower than the phase velocity of the mode at the difference frequency. Note that for GaAs $\lambda_c \approx 1.35$ μm [8].

In GaAs-based waveguides, to ensure the phase-matching condition for $\lambda < \lambda_c$, it was proposed to use as a pump a high-order mode for a shorter wavelength and a fundamental mode for a longer wavelength. The feasibility of this approach was confirmed in laser diodes with a composite resonator, in which the generation of the difference frequency in the mid-IR range with wavelengths of 8, 8.8 and 11.7 μm was obtained [9, 10]. However, the use of different-order modes in the near-IR range to achieve phase-matching conditions is inefficient for generating a difference frequency in the THz frequency range due to the small overlap integral of different-order modes in the near-IR range [11]. The problem of satisfying the phase-matching conditions for the two fundamental near-infrared modes in GaAs-based lasers with InGaAs quantum wells is related to the impossibility of using In-containing quantum wells (due to the strong mismatch of the GaAs and InAs lattice constants) to expand the near-IR wavelength range down to the required 1.35 microns.

Several designs of interband GaAs-based lasers with an emission wavelength of ~1 μm were also proposed and theoretically investigated, in which the phase matching condition can be satisfied for two fundamental near-IR modes [12–14]. However, the use of a plasma waveguide [12, 13] or a metal grating [14] significantly reduces the efficiency of difference-frequency generation due to strong absorption of radiation by free carriers in the range of 1–5 THz.

In contrast to GaAs, in HgCdTe structures with a low Hg content, the phase-matching condition is satisfied at wavelengths of the two fundamental modes of the near-IR range greater than 1 μm [7]. The nonlinear susceptibility of CdTe (~167 pm V^{-1}) is comparable to that of GaAs [15]. In addition, the lattice constants of HgTe and CdTe are very close, which allows the formation of HgTe/CdTe quantum wells. Solid cadmium–mercury–tellurium solutions (MCT, or CdHgTe) have been studied for more than four decades, and over the years much data has been accumulated on the preparation technology and properties of these compounds, in which the bandgap width can be varied within wide limits from 0 to 1.45 eV by changing the composition. This material is widely used to make detector and detector matrices of the mid-IR range (see, e.g., [16] and references therein). Lasers based on HgCdTe have also been known for a long time [17]. Until recent time they generated radiation with a wavelength of up to 5.4 μm at a cryogenic temperature [18] and up to 2.2 μm at room temperature [19].

In recent years, due to the qualitative leap in the technology of molecular beam epitaxy (MBE) of such structures in a number of technological groups, the problem of producing

A.A. Dubinov, V.Ya. Aleshkin, S.V. Morozov Institute for Physics of Microstructures, Russian Academy of Sciences, ul. Akademicheskaya 7, Afonino, 603087 Kstovsky district, Nizhny Novgorod region, Russia; e-mail: sanya@ipm.sci-nnov.ru

Received 2 November 2018; revision received 25 January 2019
Kvantovaya Elektronika **49** (7) 689–692 (2019)
Translated by V.L. Derbov

THz sources has a good perspective, as shown by recent experimental results. In particular, in HgCdTe-based lasers with narrow-bandgap HgTe/HgCdTe quantum wells, stimulated emission was first observed under optical pumping up to a wavelength of 20 μm (above 15 THz) at a cryogenic temperature [20, 21]. At higher temperatures, Auger recombination prevents generation in such narrow-bandgap layers [22, 23]. The latest results on the observation of stimulated radiation in waveguide structures based on HgTe/CdHgTe quantum wells at temperatures increased up to 265 K (13 °C) for a wavelength of 2.87 μm [24] show that there are reasonable prospects for fabricating interband lasers based on such structures, emitting in the wavelength range 1.5–3 μm and operating at room temperature.

In this paper, the generation of THz radiation at a difference frequency in a HgCdTe-based laser with HgTe quantum wells is theoretically investigated. It is shown that in a such laser with a waveguide width of 100 μm and the near-IR radiation power about 1 W, the power of radiation at the difference frequency in the range of 0.5–3.5 THz reaches 90 μW at room temperature.

2. Laser design

To generate radiation at the difference frequency, it is proposed to use a two-chip laser with a composite resonator consisting of two single-frequency continuous-wave quantum-well lasers oscillating at two frequencies in the near-IR range, mounted on a single heatsink in close proximity to each other. In this scheme, both lasers generate a fundamental transverse mode. The radiation of one laser is introduced into the waveguide of the other (normal to the transverse edge of the waveguide) and the frequency equal to the difference between the oscillation frequencies of these lasers is generated. Such a design allows introducing a noticeable part (~40%) of the radiation power of one laser into another [9, 10].

For HgCdTe laser emitting a difference frequency, the following design is proposed based on the traditional design of laser structures [24]. An undoped CdTe buffer layer with a thickness of 4 μm and then an n-CdTe 1 μm thick layer (carrier concentration 10^{17} cm^{-3}) are grown on a semi-insulating GaAs 400 μm thick substrate [plane (0, 1, 3)]. These layers play the role of confinement and injection layers in the laser. Then a waveguide undoped $Hg_{0.2}Cd_{0.8}Te$ layer with a thickness of 1 μm is grown for modes with a wavelength of ~1.55 μm and a thickness of 1.5 μm for modes with a wavelength of 3 μm. One or a few HgTe quantum wells with a thickness determined by the wavelength of the fundamental interband optical transition, calculated in the Kane 8×8 model [25], should be located in the waveguide layer. For a wavelength of 1.55 μm at room temperature, the thickness of the $HgTe/Hg_{0.2}Cd_{0.8}Te$ quantum well is 0.8 nm (or 10 nm for the $Hg_{0.42}Cd_{0.58}Te/Hg_{0.2}Cd_{0.8}Te$ quantum well); for a wavelength of 3 μm at a temperature of 250 K, the thickness of the $HgTe/Hg_{0.2}Cd_{0.8}Te$ quantum well is 2 nm. The contact and confinement p-CdTe 0.5 μm thick layers (carrier concentration 10^{17} cm^{-3}) should be placed on top of the waveguide layer. Next, a metallic (Au) contact is applied.

3. Computational model

In materials with a zinc blende structure (T_d crystal symmetry), the second-order nonlinear dielectric susceptibility tensor $\chi^{(2)}_{ijk}$ is symmetric with respect to the permutation of indices in the coordinate system, where the axes x', y', z' are directed along the crystallographic axes [1, 0, 0], [0, 1, 0], [0, 0, 1], respectively [6]. In addition, only the components with all three indices unequal to each other are nonzero. Therefore, this tensor can be described by a single function of frequency: $\chi^{(2)}_{x'y'z'} = \chi^{(2)}$.

In the general case, the components of the nonlinear polarisation in the coordinate system x', y', z' can be presented as follows:

$$\begin{aligned} P_{x'} &= \chi^{(2)}(E_{1y'}E_{2z'} + E_{2y'}E_{1z'}),\\ P_{y'} &= \chi^{(2)}(E_{1x'}E_{2z'} + E_{2x'}E_{1z'}),\\ P_{z'} &= \chi^{(2)}(E_{1y'}E_{2x'} + E_{2y'}E_{1x'}), \end{aligned} \tag{1}$$

where E_{ji} is the ith component of the electric field of the near-IR mode, and j is the number of the near-IR mode with the frequency ω_j, respectively.

In the case when the laser structure is grown in the plane (0, 1, 3), let us choose a new coordinate system with axes x, y, z, which is rotated by an arbitrary angle φ around the axis $z \parallel (0, 1, 3)$. When $\varphi = 0$, the x axis coincides with the direction [1, 0, 0]. Let the near-IR modes have TE polarisation and propagate along the x axis. Then, only one y-component of the electric field of the near-IR modes will be nonzero:

$$\begin{aligned} E_j(x,z,t) = A_j(z)[&\exp(\mathrm{i}k_{jx}x - \mathrm{i}\omega_j t)\\ &+ \exp(-\mathrm{i}k_{jx}x + \mathrm{i}\omega_j t)], \end{aligned} \tag{2}$$

where k_{jx} is the x-component of the wave vector of the jth near-IR mode.

It follows that

$$\begin{aligned} E_{jx'} &= -E_j(x,z,t)\sin\varphi,\\ E_{jy'} &= \frac{3}{\sqrt{10}}E_j(x,z,t)\cos\varphi,\\ E_{jz'} &= -\frac{1}{\sqrt{10}}E_j(x,z,t)\cos\varphi, \end{aligned} \tag{3}$$

and the nonlinear polarisation components in the new coordinate system will take the form

$$\begin{aligned} P_x &= \frac{3}{5}\chi^{(2)}\cos\varphi(3\sin^2\varphi - 1)E_1(x,z,t)E_2(x,z,t),\\ P_y &= \frac{9}{5}\chi^{(2)}\cos^2\varphi\sin\varphi E_1(x,z,t)E_2(x,z,t),\\ P_z &= -\frac{8}{5}\chi^{(2)}\cos\varphi\sin\varphi E_1(x,z,t)E_2(x,z,t). \end{aligned} \tag{4}$$

Therefore, a wave at the difference frequency can have both TE and TM polarisation. However, due to the fact that in this laser the separation between the metal contact and the waveguide for near-IR modes is much smaller than the wavelength of difference-frequency radiation, the overlap between the near-IR modes and the difference-frequency TE mode will be small, since the TE mode has only the tangential electric field component, which is very small in the metal. Conversely,

the TM-mode component of the electric field normal to the surface of the metal contact has a maximum near the metal surface. Therefore, below we consider only the TM mode at the difference frequency. Then the equation for the y-component of the magnetic field of the difference-frequency wave has the form

$$\varepsilon(z)\frac{\partial}{\partial z}\left[\frac{1}{\varepsilon(z)}\frac{\partial H_y'(x,z,t)}{\partial z}\right]+\frac{\partial^2 H_y'(x,z,t)}{\partial x^2}-\frac{\varepsilon(z)}{c^2}\frac{\partial^2 H_y'(x,z,t)}{\partial t^2}$$
$$=\frac{4\pi}{c}\frac{\partial}{\partial t}\left\{\varepsilon(z)\frac{\partial}{\partial z}\left[\frac{P_x}{\varepsilon(z)}\right]-\frac{\partial P_z}{\partial x}\right\}, \quad (5)$$

where $\varepsilon(z)$ is the dielectric constant. With Eqns (2) and (4) taken into account, the first term in the right-hand side of Eqn (5) is odd with respect to z and close to zero when integrated within symmetric limits (we will neglect this term below). Then the value of $|P_z|$ should be maximal for the angle $\varphi = \pi/4$ and $P_z = -0.8\chi^{(2)}E_1(x, z, t)E_2(x, z, t)$. Thus, from the point of view of the amplitude of the electromagnetic field at the difference frequency, the most optimal will be the propagation of the near-IR modes at an angle of 45° between the coordinate axes [1,0,0] and $[0, 3, \bar{1}]$.

Obviously, the solution of Eqn (5) can be represented as twice the real part of the solution of an equation similar to Eqn (5), which has only one exponent in the right-hand side: $H_y'(x, z, t) = 2\mathrm{Re}[H_y(x, z, t)]$. In the approximation $\alpha L \gg 1$ (α is the absorption coefficient at the difference frequency, and L is the laser length), which will be validated below, one can search for a solution in the form $H_y(x, z, t) = H_y(z)\times \exp(ik_x x - i\omega t)$, where $k_x = k_{2x} - k_{1x}$. Then the equation for $H_y(z)$ can be written as

$$\varepsilon(z)\frac{\mathrm{d}}{\mathrm{d}z}\left[\frac{1}{\varepsilon(z)}\frac{\mathrm{d}H_y(z)}{\mathrm{d}z}\right]+\left[\varepsilon(z)\frac{\omega^2}{c^2}-k_x^2\right]H_y(z)$$
$$=\frac{16\pi}{5}\frac{k_x\omega}{c}\chi^{(2)}(\omega)\,A_1(z)A_2(z). \quad (6)$$

At the interface between layers with different dielectric constants, $H_y(z)$ and $\varepsilon^{-1}(z)(\mathrm{d}H_y/\mathrm{d}z)$ are continuous. To find the right-hand side of Eqn (6), it is necessary to solve the equations for the TE modes of the near-IR range:

$$\frac{\mathrm{d}^2A_j(z)}{\mathrm{d}z^2}+\left[\frac{\varepsilon(z,\omega_j)\omega_j^2}{c^2}-k_{jx}^2\right]A_j(z)=0. \quad (7)$$

At the boundary of layers with different dielectric constants, $A_j(z)$ and $\mathrm{d}A_j(z)/\mathrm{d}z$ are continuous. The boundary conditions for waveguide modes are given by the requirements $A_j(z) \to 0$ when $z \to \pm\infty$.

The electric field component of the difference-frequency mode $E_z(z)$ and its power are determined from the expressions (in which L_y is the width of the laser waveguide)

$$E_z(z)=\frac{1}{\varepsilon(z)}\left[\frac{16\pi}{5}\chi^{(2)}A_1(z)A_2(z)-\frac{ck_x}{\omega}H_y(z)\right],$$
$$P=-\frac{cL_y}{2\pi}\int_{-\infty}^{\infty}\mathrm{Re}\,(H_y(z)E_z^*(z))\,\mathrm{d}z. \quad (8)$$

In the calculation, we used frequency dependences of the refractive index of GaAs and $Hg_xCd_{1-x}Te$ layers for near-IR modes from [26] and [27], respectively. The complex dielectric constants of GaAs and $Hg_xCd_{1-x}Te$ layers in the THz frequency range were calculated taking into account the contributions of carriers (within the Drude model) and polar-optical phonons [12, 28] using data from Refs [26, 29, 30]. To calculate the complex dielectric constant of gold, the data from the reference book [31] were interpolated.

4. Results and conclusions

The calculated power and distribution of the difference-frequency mode electric field in the structure under consideration (at the power 1 W of the near-IR mode) are shown in Figs 1–3. In the calculations, the longest wavelength (λ_1 = 1.55 and 3 μm) for the modes of the near- and mid-IR range was fixed, while the variation in the difference frequency was achieved by changing the wavelength of another mode of the near- or mid-IR range. The dependence of power on the difference frequency has the form of multiple densely spaced resonant peaks. Each of them corresponds to a transverse THz waveguide mode (see Figs 1 and 2), for which the condition of equality of its phase velocity and the phase velocity of the nonlinear polarisation wave is satisfied (the role of THz waveguide is played by the entire structure).

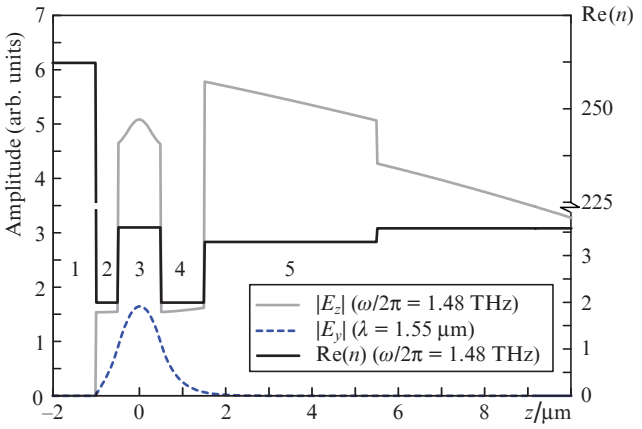

Figure 1. Moduli of the transverse electric field components of (dashed curve) the near-IR TE modes, (grey curve) the difference-frequency TM wave, and (black curve) the refractive index vs. the z coordinate for the frequency 1.48 THz (λ_1 = 1.55 μm). Layers: 1 – Au, 2 – p-CdTe, 3 – $Hg_{0.2}Cd_{0.8}Te$, 4 – n-CdTe, 5 – CdTe, 6 – GaAs.

The difference in the resonant peak positions (see Fig. 3) for two values of λ_1 is due to the wavelength dependence of the refractive index in the laser structure. The decrease in power at the maximum peaks of the difference wave for the structure with λ_1 = 3 μm is associated with a decrease in the pump power density at a fixed total power and is determined by the required increase in the effective thickness of the waveguide for radiation with a wavelength of 3 μm. According to the calculations, in the HgCdTe-based laser with a waveguide width of 100 μm and 1W of power in near-IR radiation modes, the power of the difference-frequency mode can reach 90 μW in the frequency range 0.5–3.5 THz at room temperature.

Acknowledgements. This work was supported by the Russian Science Foundation (Project No. 17-12-01360).

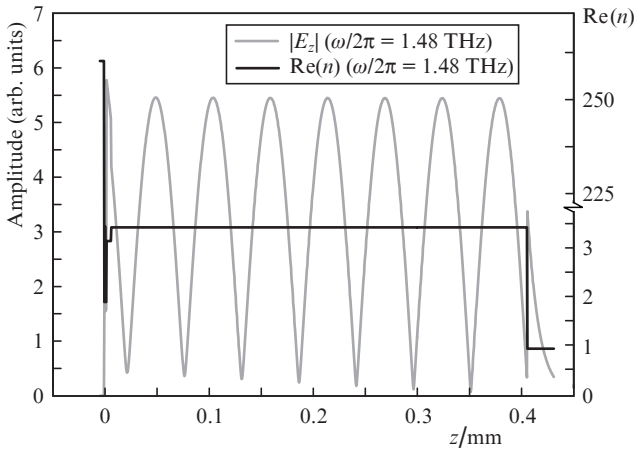

Figure 2. Modulus of (grey curve) the TM-wave electric field transverse component and (black curve) refractive index vs. the z coordinate for a frequency of 1.48 THz (λ_1 = 1.55 μm).

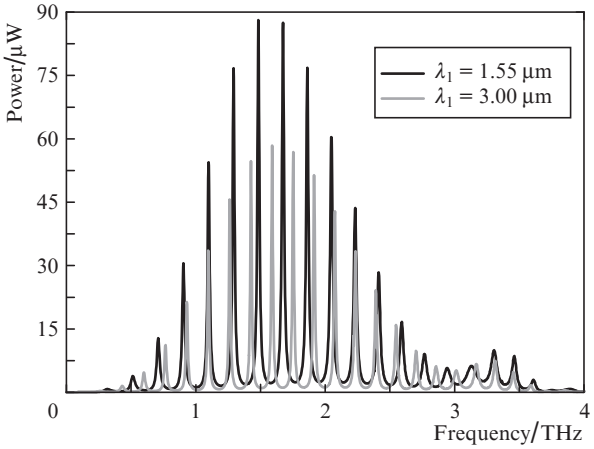

Figure 3. Frequency dependence of the radiation power at the difference frequency for two values of λ_1.

References

1. Neumaier P.F.-X., Schmalz K., Borngraber J., Wylde R., Hubers H.-W. *Analyst*, **140**, 213 (2015).
2. Hochrein T. *J. Infrared. Milli. Terahz. Waves*, **36**, 235 (2015).
3. Smolyanskaya O.A., Kravtsenyuk O.V., Panchenko A.V., Odlyanitskiy E.L., Guillet J.P., Cherkasova O.P., Khodzitsky M.K. *Quantum Electron.*, **47**, 1031 (2017) [*Kvantovaya Elektron.*, **47**, 1031 (2017)].
4. Vitiello M.S., Scalari G., Williams B., De Natale P. *Opt. Express*, **23**, 5167 (2015).
5. Aleshkin V.Ya., Afonenko A.A., Zvonkov N.B. *Semiconductors* **35** (10), 1203 (2001) [*Fiz. Tekh. Poluprovodn.*, **35**, 1256 (2001)].
6. Flytzanis C. *Phys. Rev. B*, **6**, 1264 (1972).
7. Nagai M., Tanaka K., Ohtake H., Bessho T., Sugiura T., Hirosumi T., Yoshida M. *Appl. Phys. Lett.*, **85**, 3974 (2004).
8. Berger V., Sirtori C. *Semicond. Sci. Technol.*, **19**, 964 (2004).
9. Zvonkov B.N., Biryukov A.A., Ershov A.V., Nekorkin S.M., Aleshkin V.Ya., Gavrilenko V.I., Dubinov A.A., Maremyanin K.V., Morozov S.V., Belyanin A.A., Kocharovsky V.V., Kocharovsky V.V. *Appl. Phys. Lett.*, **92**, 021122 (2008).
10. Zvonkov N.B., Biryukov A.A., Nekorkin S.M., Aleshkin V.Ya., Gavrilenko V.I., Dubinov A.A., Maremyanin K.V., Morozov S.V. *Semiconductors*, **43** (2), 208 (2009) [*Fiz. Tekh. Poluprovodn.*, **43**, 220 (2009)].
11. Aleshkin V.Ya., Dubinov A.A. *Quantum Electron.*, **38**, 149 (2008) [*Kvantovaya Elektron.*, **38**, 149 (2008)].
12. Afonenko A.A., Aleshkin V.Ya., Dubinov A.A. *Semiconductors*, **38** (2), 239 (2004) [*Fiz. Tekh. Poluprovodn.*, **38**, 244 (2004)].
13. Aleshkin V.Ya., Afonenko A.A., Biryukov A., Gavrilenko V.I., Dubinov A.A., Kocharovsky Vl.V., Morozov S.V., Maremynin K.V., Nekorkin S.M., Zvonkov B.N., Zvonkov N.B. *Acta Physica Polonica A*, **107**, 7 (2005).
14. Afonenko A.A., Aleshkin V.Ya., Dubinov A.A. *Semicond. Sci. Technol.*, **20**, 357 (2005).
15. Akitt D.P., Johnson C.J., Coleman P.D. *IEEE J. Quantum Electron.*, **6**, 496 (1970).
16. Rogalski A. *Rep. Prog. Phys.*, **68**, 2267 (2005).
17. Melngailis I., Strauss A.J. *Appl. Phys. Lett.*, **8**, 179 (1966).
18. Arias J.M., Zandian M., Zucca R., Singh J. *Semicond. Sci. Technol.*, **8**, S255 (1993).
19. Roux C., Hadji E., Pautrat J.-L. *Appl. Phys. Lett.*, **75**, 1661 (1999).
20. Morozov S.V., Rumyantsev V.V., Kadykov A.M., Dubinov A.A., Kudryavtsev K.E., Antonov A.V., Mikhailov N.N., Dvoretskii S.A., Gavrilenko V.I. *Appl. Phys. Lett.*, **108**, 092104 (2016).
21. Morozov S.V., Rumyantsev V.V., Fadeev M.A., Zholudev M.S., Kudryavtsev K.E., Antonov A.V., Kadykov A.M., Dubinov A.A., Mikhailov N.N., Dvoretsky S.A. Gavrilenko V.I. *Appl. Phys. Lett.*, **111**, 192101 (2017).
22. Krishnamurthy S., Berding M.A., Yu Z.G. *J. Electron. Mater.*, **35**, 1369 (2006).
23. Jozwikowski K., Kopytko M., Rogalski A. *J. Appl. Phys.*, **112**, 033718 (2012).
24. Fadeev M.A., Rumyantsev V.V., Kadykov A.M., Dubinov A.A., Antonov A.V., Kudryavtsev K.E., Dvoretskii S.A., Mikhailov N.N., Gavrilenko V.I., Morozov S.V. *Opt. Express*, **26**, 12755 (2018).
25. Novik E.G., Pfeuffer-Jeschke A., Jungwirth T., Latussek V., Becker C.R., Landwehr G., Buhmann H., Molenkamp L.W. *Phys. Rev. B*, **72**, 035321 (2005).
26. Madelung O. *Semiconductors: Data Handbook* (New York: Springer-Verlag, 2003).
27. Kucera Z. *Phys. Status Solidi A*, **100**, 659 (1987).
28. Ferrini R., Guizzetti G., Patrini M., Parisini A., Tarricone L., Valenti B. *Europ. Phys. J. B*, **27**, 449 (2002).
29. Danielewicz E.J., Coleman P.D. *Appl. Opt.*, **13**, 1164 (1974).
30. Baars J., Sorger F. *Solid State Commun.*, **10**, 875 (1972).
31. Palik E.D. *Handbook of Optical Constants of Solids* (New York: Academic Press, 1998).